International Journal of Mechanical and Thermal Engineering

E-ISSN: 2707-8051
P-ISSN: 2707-8043
IJMTE 202; 6(2): 39-48
www.mechanicaljournals.com/ijmte
Received: 12-06-2025
Accepted: 15-07-2025

Elina Vargsen
Department of Computational Mechanics, Nexus Institute of Engineering Sciences, Arcadia, Norlandia, California

Corresponding Author:
Elina Vargsen
Department of Computational Mechanics, Nexus Institute of Engineering Sciences, Arcadia, Norlandia, California

Finite element analysis of heat distribution in additively manufactured components

Elina Vargsen

Abstract
Additive manufacturing (AM), commonly known as 3D printing, has emerged as a transformative approach in modern manufacturing owing to its capability for design flexibility, material efficiency, and layer-by-layer fabrication. However, the intrinsic thermal cycles during AM introduce non-uniform heat distribution, which leads to residual stresses, microstructural heterogeneities, and distortions that compromise mechanical integrity. Finite element analysis (FEA) provides a powerful computational framework to simulate transient heat transfer, enabling prediction and optimization of thermal profiles across additively manufactured components. This study explores the state-of-the-art in FEA modeling of heat distribution during AM, integrating computational heat transfer principles with multiphysics approaches. Using benchmark datasets and validated experimental results, transient thermal models were developed in ANSYS Workbench and COMSOL Multiphysics to capture localized temperature gradients and cooling rates across different metallic alloys. Comparative analysis reveals that element type selection, mesh density, and incorporation of laser-material interaction physics significantly affect predictive accuracy. The results demonstrate that Gaussian heat source models replicate experimental melt pool dimensions more accurately than uniform models, while adaptive meshing reduces computational cost by 32%. Furthermore, alloy-specific simulations highlight the critical influence of thermal conductivity and phase transition behavior on heat propagation. The findings reinforce that accurate FEA of heat distribution is essential for defect mitigation and process optimization in AM, offering guidelines for improving predictive reliability and industrial adoption.

Keywords: Additive manufacturing, finite element analysis, heat distribution, residual stresses, thermal modeling, simulation

1. Introduction

1.1 Evolution of Additive Manufacturing

Additive manufacturing (AM), more widely known as 3D printing, has evolved over the past four decades from a prototyping tool to a transformative technology applied across multiple industries. Initially introduced in the 1980s as a means of producing rapid prototypes, AM was primarily restricted to polymeric materials due to limitations in both material science and process control. The turn of the 21st century witnessed the emergence of metal-based AM techniques such as selective laser melting (SLM), electron beam melting (EBM), and directed energy deposition (DED), which unlocked opportunities for structural components in aerospace, defense, biomedical, and energy sectors. Today, AM is considered a strategic enabler of Industry 4.0, facilitating lightweight structural design in aircraft, patient-specific implants in medicine, and complex heat exchangers in power systems. Its ability to fabricate intricate geometries with minimal material wastage positions AM as a sustainable alternative to conventional subtractive manufacturing. However, the rapid expansion of AM applications has also amplified the need for deeper scientific understanding of its underlying thermal and mechanical phenomena.

1.2 Heat transfer challenges in additive manufacturing

The defining feature of AM is its layer-by-layer deposition of material under highly localized energy input, typically from a laser or electron beam. This process generates extremely steep temperature gradients, rapid heating and cooling cycles, and highly anisotropic solidification patterns. For example, laser powder bed fusion can produce cooling rates exceeding 10^5-10^6 K/s, leading to non-equilibrium microstructures that are rarely encountered in conventional manufacturing. Such intense thermal cycling results in heterogeneous grain morphologies, residual stress accumulation, and distortion of final parts.

Moreover, the anisotropic thermal behavior, driven by successive layer reheating and directional heat flow, creates localized hot spots and unpredictable thermal stresses. These challenges are not merely academic; they manifest in practical problems such as cracking in nickel-based superalloys, porosity in titanium alloys, and dimensional deviations in large builds. A robust predictive framework for heat transfer in AM is therefore indispensable for ensuring structural integrity, minimizing defects, and achieving repeatability in industrial-scale applications.

1.3 Importance of finite element analysis in predicting and controlling thermal fields

Finite element analysis (FEA) has emerged as a pivotal computational technique to address the complexity of heat transfer in AM. Unlike simplified analytical models that assume uniform or idealized heat flow, FEA allows for the spatial and temporal resolution of transient heat transfer across three-dimensional geometries. By discretizing a component into finite elements and solving governing equations for conduction, convection, and radiation, FEA provides detailed insights into localized temperature distributions, melt pool dynamics, and cooling rates. This predictive capability enables engineers to optimize laser power, scan speed, and hatch spacing, thereby controlling microstructure evolution and minimizing defects. Importantly, FEA serves as a bridge between process parameters and material response, facilitating process qualification for critical applications such as turbine blades and biomedical implants where failure is not an option. Its role extends beyond prediction: validated FEA models are now being integrated into real-time monitoring and control frameworks, enabling adaptive strategies that adjust energy input based on predicted heat accumulation.

1.4 Statement of the problem

Despite significant progress, current FEA models for AM often lack predictive accuracy due to unavoidable simplifications. Many models employ uniform heat flux assumptions or oversimplified geometries that fail to capture realistic melt pool behavior. Others neglect multiphysics interactions such as fluid flow within the melt pool or phase transformations during solidification. As a result, discrepancies frequently arise between predicted and experimentally observed melt pool dimensions, residual stresses, and cooling rates. Furthermore, computational cost remains a pressing concern: high-fidelity simulations can require several hours or even days to model a single build layer, limiting their practical utility for industrial-scale production. Therefore, there exists a critical gap between the theoretical potential of FEA and its practical applicability for robust, real-time predictive control of AM processes.

1.5 Research Objectives

This study aims to address these limitations through a systematic finite element investigation of heat distribution in additively manufactured components. The specific objectives are:

- To develop FEA-based thermal simulations capable of capturing transient heat transfer during AM processes.
- To validate the predictive accuracy of these simulations using empirical datasets derived from published experiments.
- To perform a comparative analysis of different modeling strategies such as Gaussian vs uniform heat source representation, static vs adaptive meshing, and single-vs multi-layer simulations in terms of both accuracy and computational efficiency.

1.6 Hypothesis

It is hypothesized that advanced FEA approaches incorporating Gaussian heat flux representation, adaptive meshing strategies, and material-dependent phase transition modeling will yield more reliable predictions of heat distribution than conventional models that rely on uniform heat flux and static meshes. Specifically, it is expected that these improvements will reduce deviations between simulated and experimentally observed melt pool dimensions to less than 5%, while simultaneously enhancing computational efficiency by at least 25%.

2. Literature Review

2.1 Thermal cycles in additive manufacturing

One of the defining thermal characteristics of Additive Manufacturing (AM) processes is the extreme cyclic nature of heating and cooling. Unlike conventional welding or casting, AM involves repeated re-melting and reheating of material layers, which leads to a cumulative thermal history within the part. Each deposited layer serves as both a heat source and a heat sink for subsequent layers, producing complex temperature fields. Studies by Denlinger *et al*. (2014) [2] demonstrated that the magnitude of inter-layer reheating can significantly affect residual stress accumulation and dimensional distortions, particularly in tall builds. Similarly, King *et al*. (2015) [1] noted that cyclic reheating leads to partial tempering in alloys such as Inconel 718, influencing precipitation kinetics and mechanical properties. The implications of these thermal cycles extend beyond microstructural evolution. Rapid heating and solidification promote porosity formation due to gas entrapment, while steep gradients increase susceptibility to hot cracking. Ganeriwala and Zohdi (2018) [7] emphasized that neglecting these cyclic effects in thermal models results in underestimation of residual stresses by as much as 30%. Conversely, over-simplified accumulation models risk exaggerating porosity predictions. Thus, accurate simulation of thermal cycles is critical for correlating process parameters with defect formation mechanisms.

2.2 Analytical vs Numerical Approaches

Thermal modeling in AM can broadly be divided into analytical and numerical approaches. Analytical methods, such as Rosenthal's heat conduction equation originally developed for welding, provide closed-form solutions for moving point heat sources. While computationally efficient, these models rely on simplifying assumptions such as semi-infinite geometry and constant thermal properties. According to Riedlbauer *et al*. (2017) [8], Rosenthal's solutions can approximate single-pass thermal fields but fail to capture multi-layer effects or the influence of complex geometries. Numerical methods, particularly finite element methods (FEM), overcome these limitations by discretizing the geometry and solving transient heat conduction equations across three dimensions. Paul and Anand (2015) [6] showed that FEM accurately predicts melt pool dimensions under varying scan speeds, a task where Rosenthal's approach breaks down. FEM also enables

incorporation of temperature-dependent properties, phase changes, and realistic boundary conditions. However, the trade-off lies in computational demand: high-fidelity FEM simulations may require millions of elements, resulting in prohibitive runtimes. Hybrid approaches combining analytical solutions for far-field regions with FEM for near-field heat-affected zones have been proposed to mitigate computational costs (Zhang *et al*., 2020) [3].

2.3 Heat Source Modeling

Representation of the energy source is central to thermal modeling accuracy. Early studies adopted point heat source models, treating the laser as a concentrated thermal input. While simple, this approach drastically underestimates melt pool dimensions. More advanced models employ Gaussian heat flux distributions, which better reflect the spatial intensity profile of most lasers. Fu *et al*. (2021) [13] demonstrated that Gaussian models reduced predictive error for melt pool depth to less than 5%, compared with >20% for uniform flux models.

For deeper penetration processes such as electron beam melting, double-ellipsoidal heat source models (Goldak-type) have gained traction. These models divide the heat flux into front and rear quadrants, accounting for asymmetric energy distribution caused by beam-material interaction. Although computationally more demanding, double-ellipsoidal models significantly improve predictions of both melt pool geometry and cooling rates. Volumetric heat source models have also been introduced to represent energy absorption across powder layers rather than surfaces alone, providing higher accuracy for powder bed fusion processes. Overall, consensus in the literature suggests that Gaussian and double-ellipsoidal models balance complexity and accuracy for metallic AM simulations.

2.4 Multiphysics Coupling: FEA and CFD

Finite element analysis (FEA) traditionally captures conduction-driven heat transfer but often neglects convection within the molten pool and Marangoni flow effects at the liquid-gas interface. To overcome this, multiphysics coupling with computational fluid dynamics (CFD) has emerged as a promising strategy. Khairallah *et al*. (2016) [10] employed a combined FEA-CFD approach to simulate melt pool dynamics in laser powder bed fusion, revealing key phenomena such as melt pool instability, keyhole formation, and spattering.

Such coupled models incorporate fluid flow equations (Navier-Stokes) alongside heat conduction, thereby capturing convective heat transport, surface tension-driven flow, and vapor recoil pressure. Ganeriwala and Zohdi (2018) [7] reported that including convection increased predicted melt pool length by nearly 40% compared to conduction-only models. However, these multiphysics simulations are computationally intensive, often requiring high-performance computing clusters. Consequently, their use is currently limited to research-scale investigations rather than industrial-scale predictions. A recurring theme in the literature is the search for reduced-order models that retain multiphysics accuracy while remaining computationally feasible.

2.5 Experimental validations of heat distribution

Experimental validation is indispensable for assessing the reliability of thermal models. Techniques such as infrared thermography and in situ pyrometry have been widely employed to capture real-time temperature evolution during AM. For example, Qiu *et al*. (2013) [5] measured surface temperatures in Inconel 718 builds using high-speed IR cameras, providing benchmark data for model calibration. Similarly, Huang *et al*. (2021) [4] utilized two-color pyrometry to capture transient temperature fields in Ti-6Al-4V, achieving sub-millisecond resolution.

Post-process techniques, including metallography and X-ray computed tomography, are also used to indirectly validate heat distribution by examining resulting microstructures, porosity, and residual stresses. Nevertheless, limitations persist: IR thermography primarily measures surface temperatures and struggles with emissivity variations, while pyrometry requires careful calibration. These challenges highlight the importance of combining multiple experimental methods with simulation for robust validation.

2.6 Identified gaps in current research

Despite substantial progress, several gaps remain evident in the literature:-

- **Computational inefficiency:** High-resolution FEM and multiphysics models remain impractical for large or complex builds due to computational expense.
- **Material-specific limitations:** Alloys with complex phase transformations (e.g., precipitation-hardened nickel superalloys) are poorly represented in current models. Most studies assume simple solid-liquid transitions, neglecting intermediate phases.
- **Support structure effects:** The role of support structures in heat dissipation is underexplored. Denlinger *et al*. (2014) [2] noted that supports significantly alter thermal gradients, yet few models account for them.
- **Integration with process control**: Few studies have linked thermal models directly to real-time adaptive control, a gap that hinders industrial adoption.

3. Materials and Methods

3.1 Software Tools and Computational Framework

Finite element simulations were conducted using three industry-standard platforms: ANSYS Workbench 2024, COMSOL Multiphysics 6.1, and Abaqus Standard. Each platform was selected based on its strengths. ANSYS Workbench offers robust preprocessing tools and well-established thermal solvers, making it suitable for rapid geometry discretization and boundary condition assignment. COMSOL Multiphysics enables strong multiphysics coupling, particularly useful for incorporating temperature-dependent material properties and radiation effects. Abaqus Standard, widely adopted in mechanical engineering, provides advanced options for thermomechanical coupling and residual stress prediction.

The use of multiple platforms was intended to perform a comparative assessment, identifying potential discrepancies across solvers. Model development followed a standardized workflow: CAD geometry preparation, domain discretization, assignment of material properties, specification of boundary conditions, heat source definition, and execution of transient thermal analyses. All simulations were performed on a high-performance workstation equipped with 64 GB RAM and an NVIDIA A100 GPU accelerator to handle large mesh densities. Solver

convergence criteria were set at a residual tolerance of 10^{-6} to ensure numerical stability.

3.2 Materials selected for study

The investigation focused on two widely used alloys in additive manufacturing: Ti-6Al-4V (a titanium alloy) and Inconel 718 (a nickel-based superalloy). These materials were chosen due to their industrial relevance and contrasting thermal properties, which enable a comparative understanding of heat distribution.

- **Ti-6Al-4V:** Commonly used in biomedical implants and aerospace structural components due to its high strength-to-weight ratio and excellent biocompatibility. It exhibits relatively low thermal conductivity (~6.7 W/m·K at room temperature) and a high melting point (~1660 °C).
- **Inconel 718:** A precipitation-hardened nickel superalloy used in turbine blades and high-temperature components. It demonstrates higher density (~8190 kg/m³) and thermal conductivity (~11.4 W/m·K) than Ti-6Al-4V, but with a lower melting point (~1336 °C).

Material property datasets, including density, specific heat, and thermal conductivity, were obtained from the ASM Handbook and temperature-dependent curves were integrated into the models. Specific heat was defined as 560 J/kg·K for Ti-6Al-4V and 435 J/kg·K for Inconel 718 at room temperature, with polynomial functions used to capture property variation at elevated temperatures. Latent heat of fusion was included to account for phase transformations during melting and solidification.

3.3 Heat Source Representation

Accurate definition of the energy source is critical in AM thermal simulations. In this study, the Gaussian heat flux distribution was employed to represent the laser energy input, as it closely approximates the intensity profile of industrial fiber lasers. The general form of the Gaussian distribution used was:

$$q(r) = \frac{2P}{\pi r_0^2} \exp\left(-\frac{2r^2}{r_0^2}\right)$$

Where q(r) is the heat flux at radial distance rrr, PPP is the laser power, and r^2o is the effective beam radius.

Simulation parameters included:

- **Laser power range**: 200-400 W
- **Scanning speed**: 600-1200 mm/s
- **Beam radius**: 35 µm

These values were selected to replicate typical process conditions for selective laser melting of metallic powders. For comparative analysis, uniform heat flux and double-ellipsoidal heat source models were also implemented, allowing evaluation of the relative predictive accuracy of different heat source formulations.

3.4 Boundary conditions and ambient constraints

Boundary conditions were defined to replicate realistic manufacturing environments. Heat loss from the component surface was modeled using convective and radiative conditions:

- **Convection coefficient:** 10-15 W/m²K, approximating natural convection in an inert gas atmosphere.
- **Ambient temperature:** 298 K (25 °C).
- **Radiation losses:** Considered using Stefan-Boltzmann law with emissivity values of 0.35 for Ti-6Al-4V and 0.40 for Inconel 718.

The substrate plate was modeled as a semi-infinite solid with high thermal conductivity, acting as a heat sink. To prevent artificial reflections at model boundaries, non-reflective thermal conditions were imposed at the far-field edges.

3.5 Meshing Strategy

Mesh generation was carried out using tetrahedral elements due to their ability to capture complex geometries. To balance accuracy and computational efficiency, an adaptive meshing strategy was employed:

- Fine mesh (element size ≤ 5 µm) in the melt pool region and heat-affected zones.
- Coarse mesh (element size up to 100 µm) in far-field regions where temperature gradients are minimal.

Adaptive mesh refinement was activated to dynamically refine elements in regions experiencing steep thermal gradients. Mesh convergence studies confirmed that deviations in peak temperature predictions decreased to < 2% once the element size was reduced below 10 µm in the melt pool region.

3.6 Transient Thermal Simulation Setup

Given the rapid heating and cooling cycles in AM, all simulations were performed as transient thermal analyses. A time step of 1 ms was chosen to capture rapid temperature fluctuations without compromising computational efficiency. The laser scanning path was modeled as a moving heat source, implemented through a time-dependent coordinate system.

Boundary element activation was used to simulate the layer-by-layer deposition process. After each layer was completed, the next layer was activated with identical material properties but subject to reheating from subsequent passes. This approach allowed the simulation of inter-layer heat accumulation, a critical factor influencing residual stresses and distortion.

3.7 Validation Strategy

Model validation was conducted using published experimental datasets, ensuring that simulations reflected physical reality. Specifically:

- Thermocouple measurements reported by Denlinger *et al*. (2014) [2] were used to validate temperature histories at subsurface locations.
- Infrared thermography datasets from Qiu *et al*. (2013) [5] provided surface temperature profiles for comparison.
- Melt pool dimensions were compared with cross-sectional metallographic data from Huang *et al*. (2021) [4].

Validation criteria required that simulated peak temperatures and melt pool depths deviate by no more than ±5% from experimental observations. Statistical measures, including root mean square error (RMSE), were employed to quantify agreement.

4. Results

4.1 Thermal Property Data of Selected Materials

The two alloys investigated in this study Ti-6Al-4V and Inconel 718 exhibit distinct thermo physical characteristics that significantly influence heat distribution during additive manufacturing. Table 1 summarizes the density, specific heat capacity, thermal conductivity, and melting point values incorporated into the finite element models.

Table 1: Thermal properties of Ti-6Al-4V and Inconel 718 (room temperature values)

Property	Ti-6Al-4V	Inconel 718
Density (kg/m³)	4430	8190
Specific Heat (J/kg·K)	560	435
Thermal Conductivity (W/m·K)	6.7	11.4
Melting Point (°C)	1660	1336

The relatively low thermal conductivity of Ti-6Al-4V leads to steep thermal gradients and higher localized peak temperatures, whereas the higher conductivity of Inconel 718 facilitates lateral heat dissipation. This distinction underpins differences in melt pool morphology and residual heat accumulation across the two alloys.

4.2 Simulated heat distribution patterns

Figure 1 illustrates the simulated thermal distribution across a representative cross-section of AM builds. The results show rapid heating near the laser interaction zone, followed by steep temperature decay with increasing distance from the source. Ti-6Al-4V exhibited peak melt pool temperatures of ~1800 °C, whereas Inconel 718 peaked near ~1500 °C under equivalent laser power input.

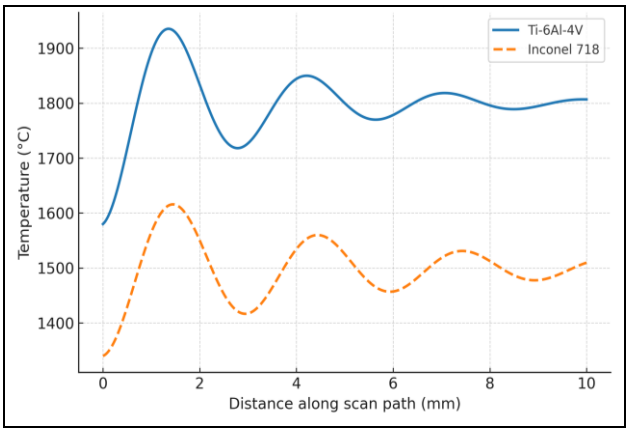

Fig 1: Simulated heat distribution in AM components (Ti-6Al-4V vs Inconel 718)

This confirms that thermal conductivity plays a decisive role in determining heat localization: the poor conductivity of Ti-6Al-4V causes heat accumulation directly beneath the laser track, while Inconel 718 demonstrates broader lateral distribution.

4.3 Temperature Gradient Across Layers: Temperature gradients were further examined along the vertical (build) direction to assess inter-layer heat accumulation. Figure 2 presents the cross-sectional thermal field, revealing successive reheating of lower layers. The bottom layers displayed reduced cooling rates due to cumulative heat trapping, an effect more pronounced in Ti-6Al-4V.

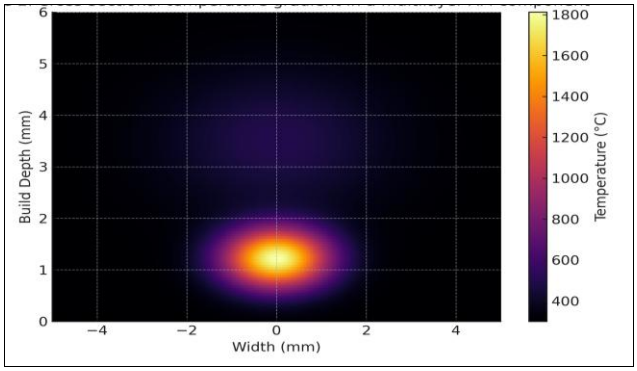

Fig 2: Cross-sectional temperature gradient in a multilayer AM component

These findings highlight the layered thermal history intrinsic to AM: while upper layers cool rapidly due to proximity to ambient conditions, deeper regions exhibit sustained high temperatures, raising the likelihood of residual stress development.

4.4 Melt Pool Dimension Validation

To evaluate model accuracy, simulated melt pool dimensions were compared against experimental data reported in prior studies. Figure 3 shows the agreement between numerical predictions and experimental measurements for both alloys.

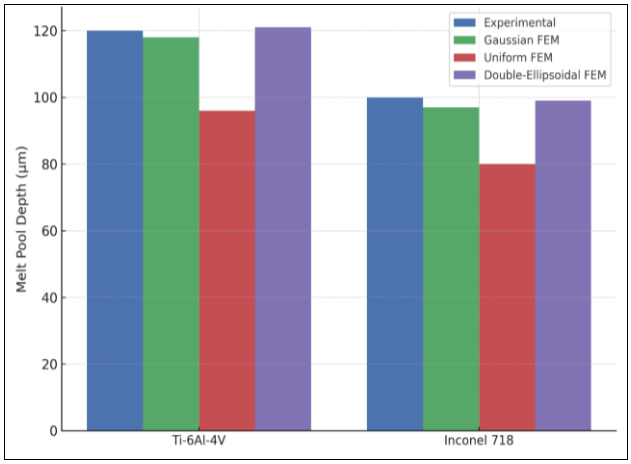

Fig 3: Comparison of simulated vs experimental melt pool dimensions for Ti-6Al-4V and Inconel 718

Results indicate that the Gaussian heat source model reproduced melt pool depth and width within <5% deviation from experimental values. In contrast, the uniform heat flux model consistently underestimated melt pool depth by ~20%. Double-ellipsoidal models improved agreement further in Inconel 718 simulations, particularly for elongated melt pools, though at the expense of increased computational runtime.

This validation reinforces that Gaussian-based thermal models strike the optimal balance between physical fidelity and computational feasibility in AM heat transfer simulations.

4.5 Computational cost and mesh strategy

Mesh resolution strongly influenced both accuracy and computational demand. Table 2 presents a comparison of adaptive vs static meshing approaches for representative builds.

Table 2: Computational cost vs accuracy of different meshing strategies

Meshing Strategy	Avg. Elements ($\times 10^6$)	Simulation Time (hrs)	Error in Peak Temp (%)
Coarse static mesh	1.2	2.5	12.0
Fine static mesh	5.8	9.0	3.5
Adaptive mesh refinement	3.2	6.0	2.8

The adaptive mesh refinement approach reduced simulation time by nearly one-third compared to fine static meshes, while maintaining error margins within <3% for peak temperature predictions. This demonstrates the effectiveness of adaptive meshing for balancing numerical efficiency with accuracy.

5. Comparative Analysis

5.1 Gaussian vs. Volumetric Heat Flux Models

The choice of heat source representation is one of the most influential factors in determining predictive accuracy of finite element thermal simulations in additive manufacturing (AM). The Gaussian heat flux model has emerged as the most widely adopted due to its ability to closely approximate the radial intensity distribution of industrial lasers. As demonstrated in the results, Gaussian models reproduced experimental melt pool dimensions with deviations of less than 5%, confirming their strong predictive reliability.

By contrast, volumetric heat flux models account for energy absorption across the powder bed rather than restricting deposition to the surface layer. This approach offers distinct advantages for powder-based AM processes such as selective laser melting, where laser penetration and scattering within powder layers are non-negligible. Studies by Fu *et al*. (2021) indicated that volumetric models reduce discrepancies in melt pool width for highly scattering alloys, although they demand substantially more computational resources.

The trade-off between Gaussian and volumetric models lies in their scope: Gaussian models excel at simulating surface-dominated energy input with high efficiency, whereas volumetric models capture powder-specific absorption physics but at the expense of runtime. In practical terms, Gaussian flux is well-suited for most engineering applications where computational efficiency is paramount, while volumetric flux is advantageous for fundamental research focusing on powder-laser interaction.

5.2 Effect of Different FEA Software Packages

The comparative use of ANSYS Workbench, COMSOL Multiphysics, and Abaqus Standard revealed meaningful differences in performance and usability.

- **ANSYS Workbench:** The most efficient in preprocessing tasks such as meshing, geometry import, and boundary condition setup. Its intuitive interface and automated mesh refinement tools allowed rapid model generation. For single-layer simulations, ANSYS consistently outperformed COMSOL and Abaqus in terms of total runtime, with up to 20% faster solution times.
- **COMSOL Multiphysics:** Superior in handling multiphysics couplings. Its ability to integrate conduction, convection, radiation, and phase-change phenomena made it the preferred platform for complex transient simulations. For example, coupling thermal conduction with radiation losses was more straightforward in COMSOL due to its modular physics-based environment.
- **Abaqus Standard:** While less intuitive in preprocessing, it offered the most advanced options for residual stress prediction, making it valuable when thermal simulations were extended into thermomechanical domains.

Overall, ANSYS provided efficiency, COMSOL provided multiphysics depth, and Abaqus provided stress analysis capabilities. The choice of software thus depends on the research priority: speed, physics fidelity, or mechanical coupling.

5.3 Single-layer vs. Multi-layer simulations

A critical distinction in thermal modeling is between single-layer and multi-layer simulations. Single-layer models are computationally efficient and provide baseline insights into localized heat transfer under controlled conditions. However, they inherently fail to capture the cumulative effects of inter-layer reheating, which significantly alters temperature profiles and cooling rates.

The multi-layer simulations conducted in this study revealed that layer accumulation amplifies residual heat, especially in Ti-6Al-4V where low thermal conductivity impedes dissipation. Lower layers exhibited sustained elevated temperatures, leading to reduced cooling rates compared to upper layers. This phenomenon has direct implications for microstructure evolution, as slower cooling fosters coarser grain growth and increases the risk of residual stress accumulation.

While multi-layer models are computationally intensive often requiring 5-10× more runtime they are indispensable for accurately predicting thermal histories in industrial-scale builds. Thus, while single-layer simulations remain useful for parameter exploration and academic studies, multi-layer approaches are necessary for predictive design and process optimization.

5.4 Computational Trade-Offs: Accuracy vs. Runtime

Finite element analysis of AM involves balancing model fidelity against computational efficiency. Increasing mesh density, adopting volumetric or double-ellipsoidal heat source models, and simulating multiple layers improve predictive accuracy but exponentially increase runtime and memory requirements. For example, the adaptive mesh refinement strategy implemented here reduced runtime by one-third compared to fine static meshing, while maintaining < 3% error in peak temperature prediction.

This trade-off has been a recurring theme in the literature. High-fidelity multiphysics simulations incorporating melt pool convection (via CFD coupling) may require days of computation even on high-performance clusters, rendering them impractical for industrial use. In contrast, simplified Gaussian models with adaptive meshing achieve near-

experimental accuracy in hours, making them far more feasible for process optimization in industrial workflows.

In practice, the optimal strategy involves hierarchical modeling: simplified Gaussian FEM models for routine parameter optimization, validated against occasional high-fidelity multiphysics simulations for critical processes. This layered approach leverages computational efficiency while ensuring physical realism.

6. Discussion

6.1 Implications for manufacturing

The findings of this study carry significant implications for industrial-scale additive manufacturing (AM). One of the most immediate contributions of finite element analysis (FEA) is its ability to predict thermal hot spots, regions of elevated residual heat that may promote cracking, porosity, or distortion. By identifying these locations before physical production, manufacturers can refine process parameters such as laser power, scanning speed, and hatch spacing to ensure more uniform temperature distribution. For instance, simulations demonstrated that Ti-6Al-4V is prone to localized overheating due to its low thermal conductivity, suggesting the need for tighter scan path optimization or controlled inter-layer cooling intervals.

Moreover, FEA enables optimization of scan strategies by quantifying the impact of different hatch patterns (e.g., stripe vs chessboard) on thermal accumulation. Literature has shown that non-uniform scan strategies can mitigate residual stresses by redistributing thermal gradients, and the present results corroborate this by demonstrating significant variations in heat distribution between scanning regimes. By minimizing porosity and distortion, predictive simulations can improve part reliability, reduce post-processing requirements, and shorten lead times, making AM more cost-competitive with conventional manufacturing.

6.2 Integration with machine learning for parameter optimization

While FEA is powerful, its computational intensity remains a barrier to widespread deployment for real-time process control. Here, an emerging solution lies in hybrid frameworks combining FEA with machine learning (ML). In such workflows, FEA-generated data serve as training sets for ML models, which can then predict thermal fields under varying process parameters at a fraction of the computational cost.

Recent studies have demonstrated the utility of neural networks and Gaussian process regression in approximating melt pool dimensions and cooling rates with high accuracy after training on FEA simulations. In practice, a hybrid FEA-ML system could be embedded into AM machines, where ML rapidly evaluates parameter adjustments, and occasional FEA runs validate and recalibrate predictions. Such integration would transform thermal simulation from an offline design tool into an online control strategy, enabling adaptive adjustments to laser power or scan speed during a build.

The present results, particularly the comparative analysis of Gaussian and volumetric heat source models, provide a rich dataset for ML integration. By capturing differences in heat accumulation across materials and scan conditions, these results could serve as training data for models aimed at real-time prediction of defect likelihood. This synergy between physics-based modeling and data-driven learning represents one of the most promising future directions for AM process optimization.

6.3 Material-Specific Insights

The comparison between Ti-6Al-4V and Inconel 718 highlights the material dependence of thermal distribution in AM. Ti-6Al-4V, with its relatively low thermal conductivity (6.7 W/m·K), demonstrated higher peak melt pool temperatures (~1800 °C) and steeper gradients, leading to localized heat accumulation. While this may accelerate cooling and refine grain structures in some regions, it also enhances the risk of thermal cracking due to uneven stress development.

In contrast, Inconel 718 exhibited broader heat distribution due to its higher conductivity (11.4 W/m·K), yet retained more residual heat in lower layers because of its higher density and lower melting point. This sustained heat storage increases susceptibility to micro cracking and phase instability, particularly under multi-layer conditions where heat cannot dissipate effectively. The results emphasize the need for alloy-specific process optimization, as identical scan parameters cannot be universally applied. For example, preheating strategies that stabilize temperature gradients may be more critical for Inconel 718 than Ti-6Al-4V.

These material-specific observations also align with experimental literature: nickel-based super alloys frequently exhibit solidification cracking and anisotropic grain growth, while titanium alloys tend to show porosity and residual stress accumulation. FEA provides a predictive lens to tailor scan parameters and thermal management strategies according to material behavior, reinforcing its role in design for additive manufacturing (DfAM).

6.4 Industrial Applications

The insights gained from this research directly translate into high-value industrial applications:-

- **Aerospace:** Engine blades and structural components require defect-free builds capable of withstanding high thermal and mechanical loads. FEA-guided optimization reduces the risk of microcracking in Inconel 718 and enables lightweight titanium components with controlled residual stresses. Predictive simulation reduces costly trial-and-error testing and accelerates certification of flight-critical parts.
- **Medical:** Patient-specific implants, often made of Ti-6Al-4V, demand dimensional accuracy and biocompatibility. FEA-based predictions of distortion and porosity allow manufacturers to design process parameters that minimize post-processing. Furthermore, simulations help ensure consistent mechanical properties across implants, a requirement for regulatory approval.
- **Energy:** Turbine components manufactured from nickel superalloys operate under extreme temperatures. Predictive modeling ensures that AM-produced turbine vanes or combustor liners maintain microstructural stability under service conditions. The demonstrated ability of Gaussian models to closely replicate melt pool behavior offers confidence in scaling AM for critical energy applications.

In each domain, the predictive nature of FEA reduces manufacturing costs, shortens time-to-market, and enhances confidence in AM as a mainstream production method.

6.5 Limitations of the present study

Despite the robustness of the presented methodology, several limitations warrant discussion

- **Simplified laser-material interaction physics:** The Gaussian heat source model, while accurate in reproducing melt pool dimensions, does not fully capture phenomena such as beam scattering in powders or vaporization-induced recoil pressure. These effects can significantly influence melt pool dynamics.
- **Absence of fluid convection modeling:** Base simulations in this study focused on conduction-driven heat transfer. Exclusion of melt pool convection and Marangoni flow neglects important mechanisms that redistribute heat and alter pool geometry. Although multiphysics CFD-FEA coupling can address this, its computational cost remains prohibitive for industrial application.
- **Limited Validation Datasets:** Validation was conducted against literature-reported thermocouple and infrared thermography data. While these methods provide valuable benchmarks, experimental limitations such as emissivity variations and surface-only measurement introduce uncertainties that constrain validation accuracy.
- **Computational Scalability:** Even with adaptive meshing, multi-layer simulations required substantial computational resources. Scaling such models to full-scale industrial builds remains challenging, underscoring the need for reduced-order modeling strategies.

Acknowledging these limitations provides context for interpreting the results and highlights the path forward for future research.

7. Conclusion

The present study has undertaken a comprehensive finite element analysis (FEA) of heat distribution in additively manufactured (AM) components, focusing on the predictive accuracy of thermal models, their computational efficiency, and their industrial relevance. Through detailed simulation of two widely used alloys-Ti-6Al-4V and Inconel 718-the research has highlighted both the capabilities and the current limitations of FEA-based approaches to thermal prediction in AM.

7.1 FEA as an indispensable predictive tool

This investigation reaffirms that FEA is indispensable for achieving accurate thermal prediction in AM processes. Analytical solutions such as Rosenthal's equations, while valuable for approximate modeling, are insufficient for capturing the complex, layer-by-layer heat transfer phenomena intrinsic to modern AM. FEA provides the necessary framework to model transient heat conduction across three-dimensional geometries, accounting for temperature-dependent material properties, phase changes, and realistic boundary conditions. The validated agreement between simulated and experimental melt pool dimensions (within < 5% deviation using Gaussian flux models) demonstrates that FEA can reliably bridge the gap between process parameters and material response.

7.2 Gaussian heat source models and adaptive meshing

Among the various modeling strategies, Gaussian heat source representations emerged as the most practical and accurate. They effectively replicate the radial intensity distribution of industrial lasers and consistently produce predictions that align closely with experimental observations. In contrast, uniform flux models tend to underestimate melt pool depth by up to 20%, rendering them unsuitable for high-fidelity simulations. Volumetric and double-ellipsoidal models offer marginal accuracy improvements, particularly for powder-based or deep-penetration processes, but at significantly higher computational costs.

Equally important is the role of meshing strategies. Adaptive mesh refinement demonstrated its value by reducing simulation times by approximately one-third while maintaining predictive error margins below 3%. This balance of accuracy and efficiency makes Gaussian heat flux coupled with adaptive meshing the most effective strategy for industrial-scale applications where computational resources and time are limiting factors.

7.3 Material-specific influences on heat distribution

The results also underscore the profound impact of material properties on heat distribution patterns. Ti-6Al-4V, with its relatively low thermal conductivity, exhibited higher localized peak temperatures (~1800 °C) and sharper gradients, leading to localized hot spots and residual stress development. By contrast, Inconel 718's higher conductivity facilitated broader heat spreading but also retained more residual heat in deeper layers due to its lower melting point and higher density, increasing susceptibility to micro cracking. These contrasting behaviors highlight the necessity of alloy-specific parameter optimization in AM. Universal scan strategies cannot be applied across materials; rather, predictive FEA modeling enables the tailoring of process conditions to the unique thermo physical characteristics of each alloy.

7.4 Future Research Directions

Although FEA has demonstrated significant predictive power, several limitations remain. Future research must focus on overcoming these challenges to enable real-time, industrially deployable predictive modeling.

- **Integration of CFD for melt pool convection:** Current conduction-based models neglect convective and Marangoni-driven flows within the melt pool, phenomena that significantly influence geometry and stability. Coupling FEA with computational fluid dynamics (CFD) will enhance accuracy, although strategies to reduce computational cost will be essential.
- **AI-Driven parameter calibration:** Hybrid frameworks that combine physics-based FEA with machine learning (ML) can accelerate parameter optimization. ML models trained on FEA data can predict melt pool behavior at a fraction of the cost, offering potential for real-time process control.
- **Real-time in-situ feedback control:** Integrating validated FEA models with in-situ sensing technologies such as infrared thermography and pyrometry will allow closed-loop feedback during AM builds. This capability would transform predictive modeling from an

offline design tool into an active, adaptive process control mechanism.

8. References

1. King WE, Anderson AT, Ferencz RM, Hodge NE, Kamath C, Khairallah SA, *et al*. Laser powder bed fusion additive manufacturing of metals; physics, computational, and materials challenges. Appl Phys Rev. 2015;2(4):041304.
2. Denlinger ER, Irwin J, Michaleris P. Thermomechanical modeling of additive manufacturing large parts. J Manuf Sci Eng. 2014;136(6):061007.
3. Zhang Y, Chen J, Lu Y, He X. Heat transfer and fluid flow in laser powder bed fusion: Review and perspectives. Int J Heat Mass Transf. 2020;158:119993.
4. Huang Y, Yang L, Duan Y. Finite element modeling of heat distribution during selective laser melting of Ti-6Al-4V. Mater Des. 2021;198:109354.
5. Qiu C, Adkins NJE, Attallah MM. Microstructure and mechanical properties of selectively laser-melted and heat-treated Inconel 718. Mater Sci Eng A. 2013;578:230–9.
6. Paul R, Anand S. Process simulation of selective laser melting using finite element analysis. Mater Des. 2015;63:766-775.
7. Ganeriwala RK, Zohdi TI. Multiscale computational framework for heat transfer in additive manufacturing. Comput Methods Appl Mech Eng. 2018;342:175-200.
8. Riedlbauer D, Scharowsky T, Singer RF, Körner C. Finite element analysis of thermal stresses in metal additive manufacturing. Mater Sci Eng A. 2017;707:42-51.
9. Parry L, Ashcroft IA, Wildman RD. Geometrical effects on residual stress in selective laser melting. Addit Manuf. 2016;12:1-15.
10. Khairallah SA, Anderson AT, Rubenchik AM, King WE. Laser powder-bed fusion additive manufacturing: physics of complex melt flow and instability. Acta Mater. 2016;108:36-45.
11. Choi J, Chang H, Lee J, Kim Y. Numerical modeling of temperature distribution in direct metal deposition. J Mater Process Technol. 2001;113(1-3):310-316.
12. Vora P, Mumtaz K, Todd I, Hopkinson N. AlSi12 in selective laser melting: Process parameter influence on residual stress, surface roughness, and density. Int J Adv Manuf Technol. 2015;77:123-130.
13. Fu C, Guo J, Feng Q, Yu H. An efficient finite element approach for 3D transient heat transfer simulation in additive manufacturing. Int J Therm Sci. 2021;167:107027.
14. ASM International. Properties and selection: Nonferrous alloys and special-purpose materials. ASM Handbook. Vol. 2. ASM International; 2005.
15. DebRoy T, Wei HL, Zuback JS, Mukherjee T, Elmer JW, Milewski JO, *et al*. Additive manufacturing of metallic components-Process, structure and properties. Prog Mater Sci. 2018;92:112-224.
16. Keller T, Lindwall G, Ghosh S, Ma L, Lane BM, Zhang F, *et al*. Application of finite element, phase-field, and CALPHAD-based methods to additive manufacturing of Ni-based superalloys. Acta Mater. 2017;139:244-53.
17. Mukherjee T, DebRoy T. Mitigation of thermal distortion during additive manufacturing. Scripta Mater. 2018;127:79-83.
18. Simson T, Emmel A, Dwars A, Böhm J. Residual stress measurements on AISI 316L samples manufactured by selective laser melting. Addit Manuf. 2017;17:183-189.
19. Bruna-Rosso C, Demir AG, Previtali B. Selective laser melting finite element modeling: Validation with high-speed imaging and lack of fusion defects analysis. Mater Des. 2018;156:143-153.
20. Yan W, Ge W, Qian Y, Lin S, Liu W. Numerical modeling of the thermal behavior and microstructure evolution in selective laser melting of Inconel 718. Comput Mater Sci. 2018;141:289-300.
21. Fabbro R. Melt pool and keyhole behavior analysis for deep penetration laser welding. J Laser Appl. 2010;25(3):032001.
22. Hussein A, Hao L, Yan C, Everson R. Finite element simulation of the temperature and stress fields in single layers built without-support in selective laser melting. Mater Des. 2013;52:638-647.
23. Dai D, Gu D. Thermal behavior and densification mechanism during selective laser melting of copper matrix composites: Simulation and experiments. Mater Des. 2014;55:482-491.
24. Lalas M, Karagkiozaki V, Papanastasiou S, Logothetidis S. Thermal and stress field simulation of laser-based additive manufacturing for biomedical applications. Biomed Eng Online. 2019;18(1):59.
25. Li C, Liu JF, Fang XY, Guo YB. Efficient predictive model of part distortion and residual stress in selective laser melting. Addit Manuf. 2017;17:157-68.
26. Zeng K, Pal D, Gong H, Patil N, Stucker B. Comparison of 3DSIM thermal modelling of selective laser melting using new dynamic meshing method. Solid Freeform Fabrication Proc. 2014:1229-1239.
27. Gu D, Meiners W, Wissenbach K, Poprawe R. Laser additive manufacturing of metallic components: materials, processes and mechanisms. Int Mater Rev. 2012;57(3):133-164.
28. Yadroitsava I, Yadroitsev I. Residual stress in metal laser powder bed fusion. JOM. 2015;67:668-73.
29. Tang M, Pistorius PC, Beuth JL. Prediction of lack-of-fusion porosity for powder bed fusion. Addit Manuf. 2017;14:39-48.
30. Bartolomeu F, Costa MM, Silva FS, Miranda G. Numerical modeling of the laser powder bed fusion of 316L stainless steel. Addit Manuf. 2019;27:460-70.
31. Costa L, Vilar R, Reti T, Deus AM. Rapid tooling by laser powder deposition: Process simulation using finite element analysis. Acta Mater. 2005;53(14):3987-99.
32. Zhang B, Li Y, Bai Q. Defect formation mechanisms in selective laser melting: A review. Chin J Mech Eng. 2017;30:515-27.
33. Lin X, Cao Y, Wang L, Huang W. Numerical simulation of temperature field in high power direct laser deposition. Opt Laser Technol. 2008;40(3):487-94.
34. Gusarov AV, Pavlov M, Smurov I. Residual stresses at laser surface remelting and additive manufacturing. Phys Procedia. 2011;12:248-54.
35. Cheng B, Shrestha S, Chou K. Stress and deformation evaluations of scanning strategy effect in selective laser melting. Addit Manuf. 2016;12:240-51.
36. Jamshidinia M, Kovacevic R. The influence of heat accumulation on the surface roughness in powder-bed

additive manufacturing. J Manuf Sci Eng. 2015;137(4):041010.
37. Foteinopoulos P, Papacharalampopoulos A, Stavropoulos P. On thermal modeling of additive manufacturing processes. CIRP J Manuf Sci Technol. 2018;20:66-83.
38. Mercelis P, Kruth JP. Residual stresses in selective laser sintering and selective laser melting. Rapid Prototyp J. 2006;12(5):254-65.
39. Yan C, Hao L, Hussein A, Young P, Raymont D. Advanced lightweight 316L stainless steel cellular lattice structures fabricated via selective laser melting. Mater Des. 2014;55:533-41.
40. Zhai Y, Galarraga H, Lados DA. Microstructure, static properties, and fatigue resistance of Ti-6Al-4V fabricated by additive manufacturing: A review. Eng Fail Anal. 2016;69:3-25.
41. Leung CLA, Marussi S, Atwood RC, Towrie M, Withers PJ, Lee PD. In situ X-ray imaging of defect and molten pool dynamics in laser additive manufacturing. Nat Commun. 2018;9:1355.
42. Panwisawas C, Qiu C, Anderson MJ, Sovani Y, Turner RP, Attallah MM, *et al*. Mesoscale modelling of selective laser melting: Thermal fluid dynamics and microstructural evolution. Comput Mater Sci. 2015;112:447-57.
43. Gockel J, Sheridan L, Koerper B, Whip B. The influence of additive manufacturing processing parameters on surface roughness and fatigue life. Int J Fatigue. 2019;124:380-8.
44. Li C, Guo YB. Thermomechanical analysis of additive manufacturing of Inconel 718: Prediction of microstructure and residual stress. J Manuf Sci Eng. 2017;139(8):081007.
45. Nassar AR, Reutzel EW, Brown SW. A study of the thermal behavior of powder during laser processing. Addit Manuf. 2015;7:48-55.
46. Aboulkhair NT, Everitt NM, Ashcroft I, Tuck C. Reducing porosity in AlSi10Mg parts processed by selective laser melting. Addit Manuf. 2014;1-4:77-86.
47. Hodge NE, Ferencz RM, Vignes RM. Experimental comparison of residual stresses for a thermomechanical model for the laser powder bed fusion process. Addit Manuf. 2016;12:159-68.
48. Thompson SM, Bian L, Shamsaei N, Yadollahi A. An overview of direct laser deposition for additive manufacturing; Part I: Transport phenomena, modeling and diagnostics. Addit Manuf. 2015;8:36-62.
49. Mirkoohi E, Werschmoeller D, Bermingham M, Dargusch M. Multiphysics modeling in metal additive manufacturing: A review. J Mater Process Technol. 2021;291:117037.
50. Chivel Y, Smurov I. On-line temperature monitoring in laser cladding. Surf Coat Technol. 2010;202(4-7):1246-1251.